

1: Introduction

The physical and chemical properties of soil dust aerosol particles fundamentally affect their interaction with climate, including

- Shortwave absorption and radiative forcing,
- Nucleation of cloud droplets and ice crystals,
- Heterogeneous formation of sulfates and nitrates on the surface of dust particles,
- Atmospheric processing of iron into bioavailable forms that increase the productivity of marine phytoplankton.

To distinguish between aerosols with different physical and chemical properties, lidar measurements are frequently used, such as

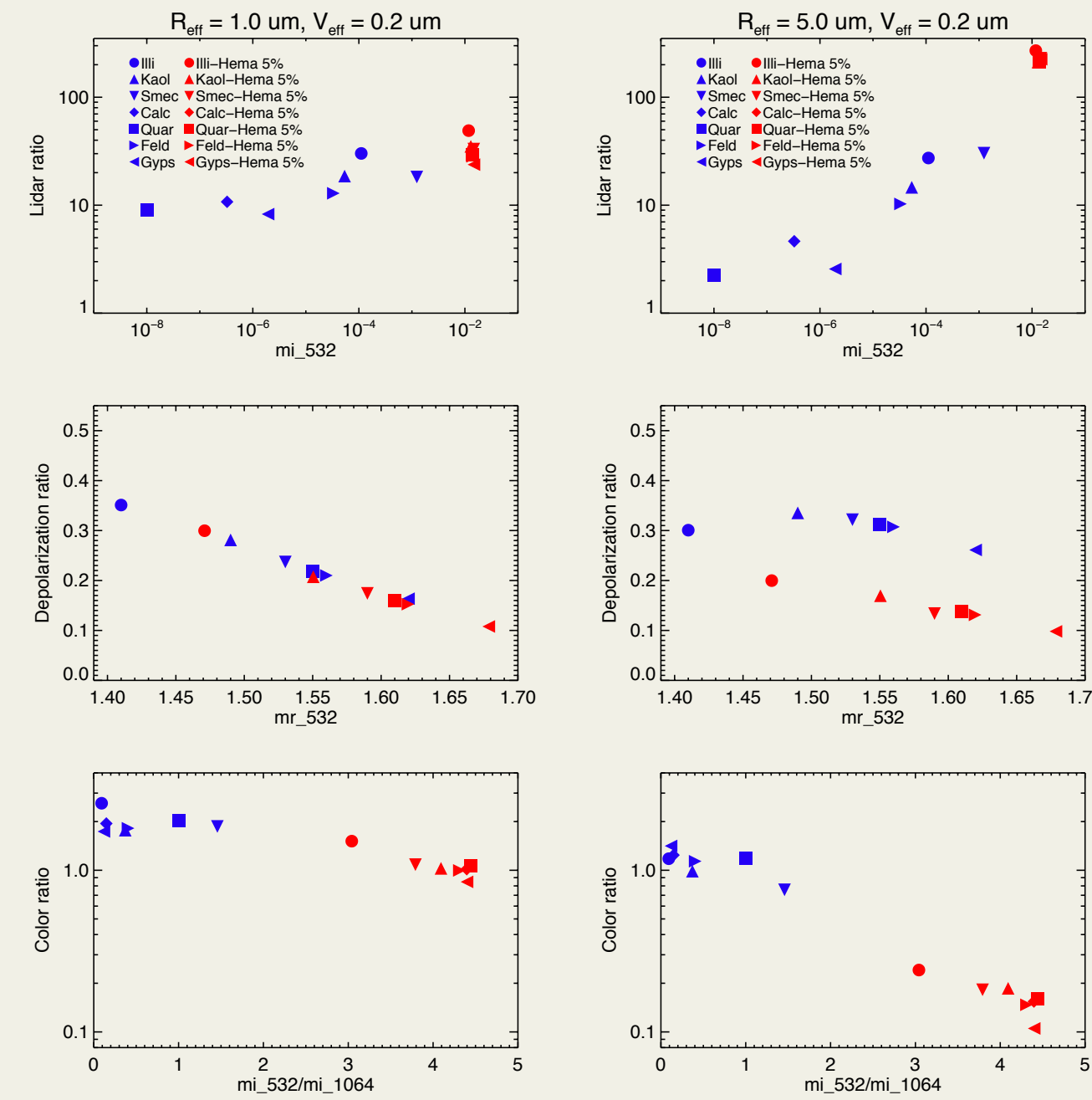
- Extinction-to-backscatter (lidar) ratio at 532 nm
- Color ratio (β_{532}/β_{1064})
- Depolarization ratio ($\beta_{\text{perpendicular}}/\beta_{\text{parallel}}$)

These lidar measurements are affected by

- Complex refractive index determined by the aerosol chemical composition
- Aerosol size distribution
- Particle shape

Here we present a study on how lidar measurements of dust aerosol at wavelengths of 532 and 1064 nm are related to size and complex refractive index. The systematic relationships between lidar observables and the dust size and complex refractive index found here that may aid the use of space-based or airborne lidars for direct retrieval of dust properties or for the evaluation of chemical transport models using forward simulated lidar variables. In addition we show preliminary forward simulations of lidar variables based on detailed modeling results

3: Lidar variables dependency on refractive index and size



Lidar ratio: Scales approximately linearly with imaginary part of refractive index on log-log scale, but slope depends on size.

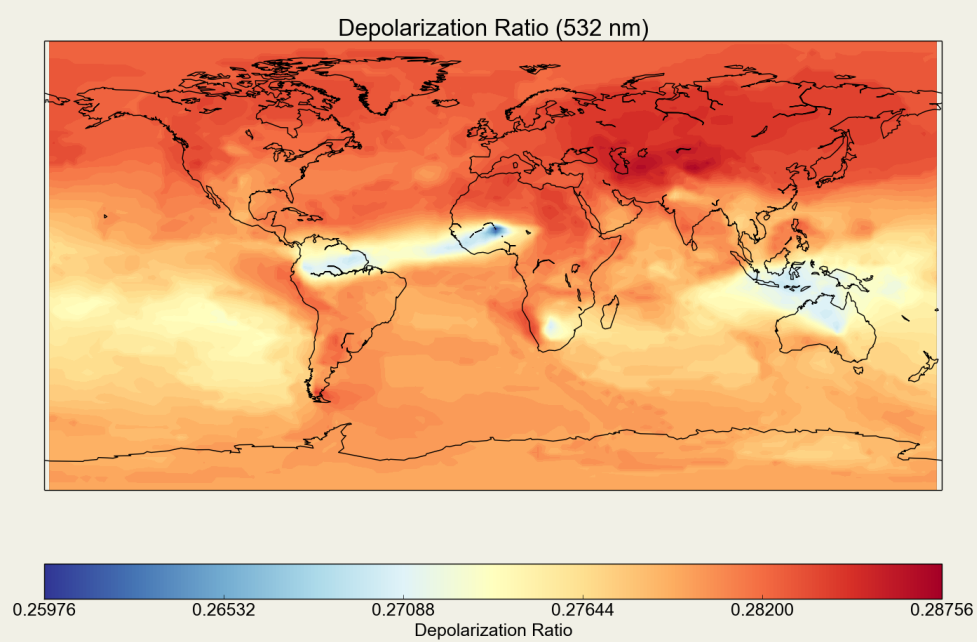
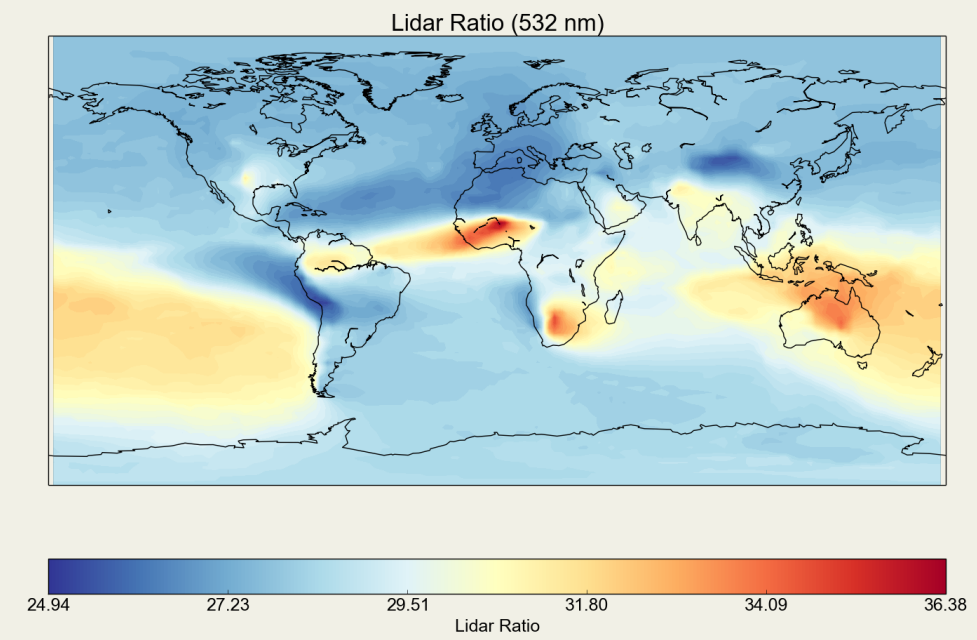
Depolarization ratio: Scales linearly with real part of refractive index for small sizes, but dependency is more complex for larger particles.

Color ratio: Scales approximately log-linearly with the ratio of imaginary part of refractive indices at the two observed wavelengths, but slope depends on size.

5: Simulated lidar results based on dust model

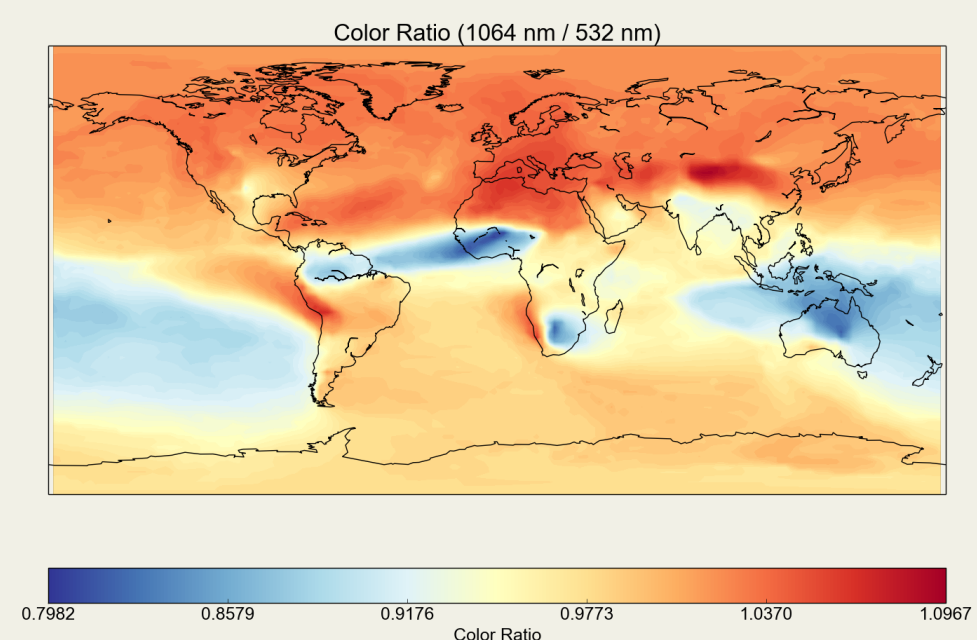
Dust model newly developed by Perlwitz et al. (ACP 2015, Part 1 and 2)

- CMIP5 version of NASA GISS Earth System ModelE2, 2x2.5 deg., 40 vertical layers
- Prognostic treatment of eight dust types in 5 size bins and treatment of iron oxides as internal mixtures
- Includes emission, advection, deposition of the minerals, turbulent mixing at surface, wet deposition by scavenging in and below clouds and condensation
- Simulations for 2002-2010, using prescribed SST and sea ice. Winds nudged using NCEP reanalyses.
- Dust properties are vertically averaged for results shown here



Lidar measurements are simulated for dust-only model runs by

1. Determining appropriate r_{eff} and v_{eff} values for each type at each grid box
2. Determining fraction of area contributed by each type at each grid box
3. Use database (panel 3) and area fractions to calculate backscatter-weighted average of lidar, depolarization and color ratios for each model grid box (cf. Burton et al., AMT, 2014).



Preliminary results (right):

- Smaller depolarization and color ratios and larger lidar ratios near Sahel and Australia, reflecting dominance of hematite-enriched koalinite and smectite, respectively.
- Relatively low lidar ratios and larger depolarization and color ratios of South American coast and in China, reflecting dominance of feldspar and illite, respectively.

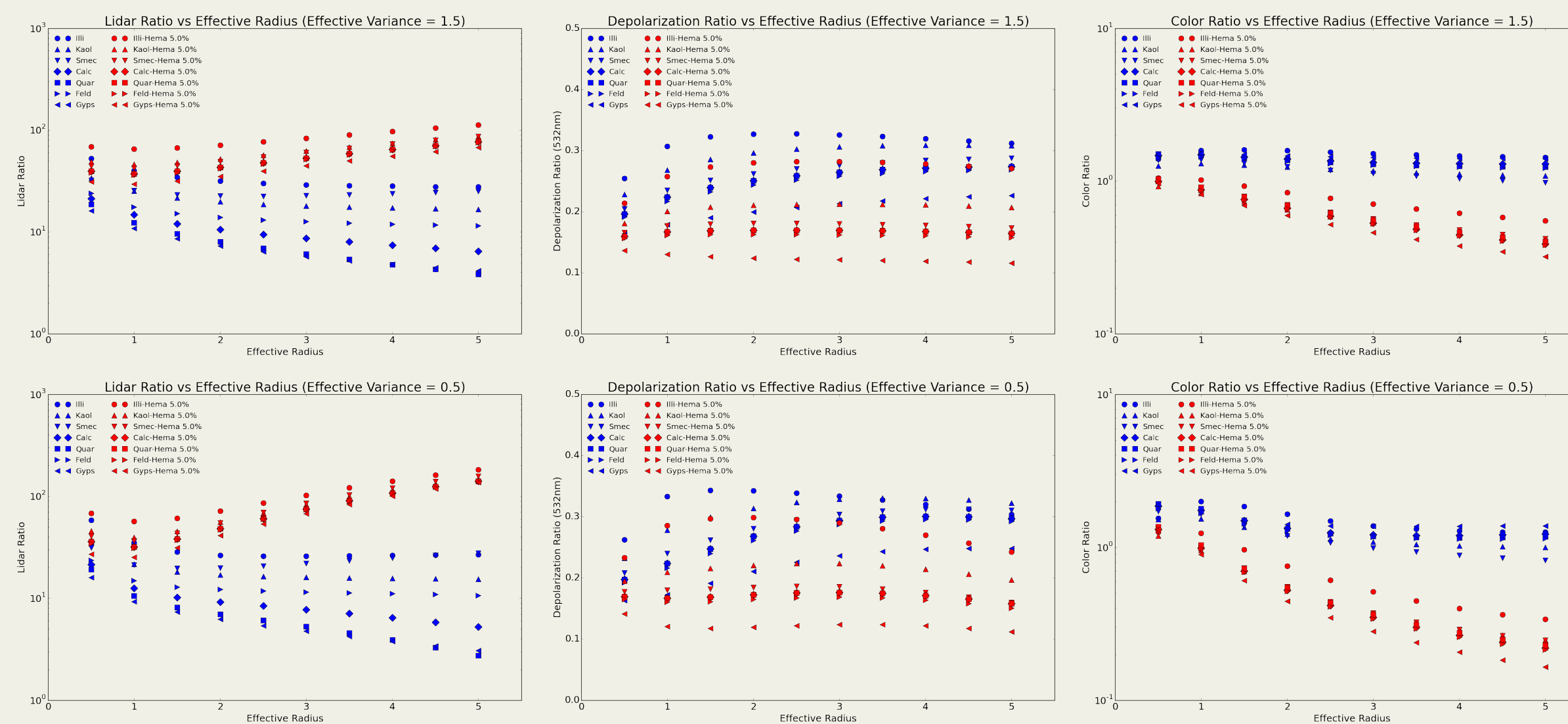
2: Mineral dust optical properties and simulations

Details of the simulations:

- Refractive index of minerals and hematite mixtures shown in table 1
- Refractive index of hematite mixtures calculated with Maxwell-Garnett mixing rule
- Optical properties derived from kernels provided by Dubovik et al. (2006)
- Assumes mixtures of spheroids with equiprobable aspect ratios between 0.5 and 2.
- Lognormal size distributions with
 - r_{eff} values from 0.5-5 μm in 10 steps and
 - v_{eff} values of 0.2, 0.5, 1, 1.5 and 2
- For minerals with refractive index values outside of the range of the optical properties database ($m_1=1.35-1.59$; $m_2=0.0005-0.02$) extrapolation is used
- Pure hematite is ignored in the simulations because of the extreme refractive indices outside the ranges of our database

		$\lambda=355 \text{ nm}$		$\lambda=532 \text{ nm}$		$\lambda=1064 \text{ nm}$	
		n	k	n	k	n	k
Pure minerals	Illite	1.41	1.48E-03	1.41	1.11E-04	1.39	1.20E-03
	Kaolinite	1.51	4.57E-04	1.49	5.38E-05	1.5	1.45E-04
	Smectite	1.54	3.98E-03	1.53	1.24E-03	1.51	8.51E-04
	Calcite	1.55	9.83E-08	1.55	3.27E-07	1.54	2.21E-06
	Quartz	1.57	1.00E-08	1.55	1.00E-08	1.53	1.00E-08
	Feldspar	1.59	3.24E-05	1.56	3.30E-05	1.55	8.17E-05
	Gypsum	1.62	5.87E-07	1.62	1.94E-06	1.62	1.62E-05
	Hematite	2.13	9.43E-01	3.07	5.42E-01	2.67	9.95E-02
Hematite mixtures	Illite + 5% Hematite	1.45	3.59E-02	1.47	1.18E-02	1.44	3.87E-03
	Kaolinite + 5% Hematite	1.55	3.80E-02	1.55	1.29E-02	1.55	3.16E-03
	Smectite + 5% Hematite	1.58	4.23E-02	1.59	1.47E-02	1.56	3.88E-03
	Calcite + 5% Hematite	1.59	3.87E-02	1.61	1.38E-02	1.59	3.13E-03
	Quartz + 5% Hematite	1.6	3.93E-02	1.61	1.38E-02	1.58	3.10E-03
	Feldspar + 5% Hematite	1.62	3.99E-02	1.62	1.40E-02	1.6	3.24E-03
	Gypsum + 5% Hematite	1.65	4.06E-02	1.68	1.48E-02	1.66	3.36E-03

4: Lidar variables dependency on size distribution



Lidar ratio: Increases with size for the highly absorbing minerals, but decrease with size for the weakly absorbing particles.

Depolarization ratio: For weakly absorbing particles, depolarization ratios increase with size. For absorbing particles this increase with size seems to be (partly) compensated by absorption.

Color ratio: For small particles, color ratios decrease with size, but asymptote to around 1 for weakly absorbing particles, while color ratios further decrease with size for absorbing particles.

6: Future work

- Extend complex refractive index and size ranges in the aerosol optical properties database
- Simulate vertically resolved lidar variables
- Calculate lidar variables for model size bins
- Add modeled non-dust aerosol to global mix
- Investigate influence of aspect ratio assumptions
- Include 335 nm wavelengths to investigate possible extra information content
- Compare with CALIPSO statistics for dusty regions

Acknowledgements

Most of the work presented here was performed by Alexander Stangl of Bergen Academies High School during the first months of his senior-year internship at NASA Goddard Institute for Space Studies